

Ternary Phase Diagrams of Alkali Bis(trifluoromethylsulfonyl)amides

Keigo Kubota, Toshiyuki Nohira, Takuya Goto, and Rika Hagiwara*

Graduate School of Energy Science, Kyoto University, Sakyo-ku, Kyoto 606-8501, Japan

Ternary phase diagrams of alkali bis(trifluoromethylsulfonyl)amides, MTf_2N ($\text{M} = \text{Li}, \text{Na}, \text{K}, \text{Cs}$), have been constructed, and their eutectic compositions and temperatures have been determined. For binary MTf_2N systems, existences of intermediate compounds, $\text{Li}_2\text{K}(\text{Tf}_2\text{N})_3$ and $\text{LiCs}(\text{Tf}_2\text{N})_2$, have been newly confirmed by X-ray diffraction, and eutectic temperatures have been revised by more precise differential scanning calorimetry.

Introduction

The authors have been exploring a new class of molten salts which possess excellent electrolyte properties at intermediate temperatures (373 to 673) K. Recently, organic solvents and room-temperature ionic liquids (RTILs) in which lithium bis(trifluoromethylsulfonyl)amide, LiTf_2N , is dissolved have been reported to possess excellent properties as electrolytes for lithium ion batteries at room temperature.^{1–5} On the other hand, the authors focused on the molten salts consisting of only alkali metal bis(trifluoromethylsulfonyl)amides, MTf_2N ($\text{M} = \text{Li}, \text{Na}, \text{K}, \text{Rb}, \text{Cs}$), from a viewpoint of the safety improvement for battery electrolytes. MTf_2N molten salt electrolytes have negligibly low vapor pressure, nonflammability, and high thermal and electrochemical stabilities. In our previous study, thermal properties of single salts and binary mixtures of MTf_2N were investigated.⁶ Single MTf_2N salts have relatively high melting temperatures except for CsTf_2N . The binary mixtures, however, were found to have much lower melting temperatures. Thus, it was concluded that the mixing of MTf_2N salts is effective to prepare molten salt electrolytes to be used at intermediate temperatures.

In this study, the thermal properties of ternary mixtures of MTf_2N salts ($\text{M} = \text{Li}, \text{Na}, \text{K}, \text{Cs}$) were systematically investigated to construct phase diagrams. Furthermore, the solid binary mixtures were studied by powder X-ray diffraction (XRD) analysis to identify intermediate compounds. Several minor revisions were also made for the eutectic temperatures of the binary mixtures which have been determined by more precise measurements.

Experimental Section

Reagents and experimental procedures are essentially the same as were reported in the previous study.⁶ Several important points and new procedures are described here. MTf_2N except for LiTf_2N were synthesized by reaction of HTf_2N and M_2CO_3 . Phase transition and thermal decomposition temperatures of MTf_2N single and mixed salts were measured by means of differential scanning calorimetry (DSC) and thermogravimetry (TG), respectively. Samples of several grams were once heated above their melting points and cooled down to room temperature by natural cooling. The obtained solids were ground into powder and subjected to DSC, TG, and XRD analyses. For all the

samples, the scanning rate was $10 \text{ K} \cdot \text{min}^{-1}$ in the first scan, and the approximate transition temperatures were determined as the points of intersection of the baseline of the DSC curve with the tangent of the endothermic peak. To determine the transition temperatures more precisely, the second scan was performed by the step heating method at intervals of 2 K for 5 min. The transition temperatures were determined in the heating process to avoid uncertainty by supercooling. The liquidus surfaces were represented in contours drawn with smooth lines by connecting melting temperatures determined by DSC. The first measurements were performed at every 10 mol % of the component salts. Further measurements were performed at every 5 mol % for the regions where the low liquidus temperatures were observed in the first measurements. In this study, composition and temperature accuracy are $\pm 1 \text{ mol } \%$ and $\pm 2 \text{ K}$.

For all samples of binary mixtures, XRD patterns were obtained using an X-ray diffractometer (Rigaku Co., Ltd. MultiFlex, $\text{Cu K}\alpha$ radiation) at room temperature. To prevent samples from absorbing moisture, the sample holder was wrapped with Parafilm (American National Can.).

Results and Discussion

Intermediate Compounds and Revised Eutectic Temperatures for Binary MTf_2N Mixed Salts. Figure 1 shows XRD charts for the solidified samples of $\text{LiTf}_2\text{N} + \text{KTf}_2\text{N}$ mixtures in the compositions of $x_{\text{LiTf}_2\text{N}} = 1.00, 0.80, 0.67, 0.40,$ and 0 . The XRD patterns of LiTf_2N are not observed at the compositions of $x_{\text{LiTf}_2\text{N}} < 0.67$. On the other hand, the patterns of KTf_2N are not observed at the compositions of $x_{\text{LiTf}_2\text{N}} < 0.67$. The patterns for the mixed salt of $(x_{\text{LiTf}_2\text{N}}, x_{\text{KTf}_2\text{N}}) = (0.67, 0.33)$ is different from those for LiTf_2N and KTf_2N . These results are reasonably explained by the formation of an intermediate compound, $\text{Li}_2\text{K}(\text{Tf}_2\text{N})_3$, at this composition.

Figure 2 shows XRD charts of $\text{LiTf}_2\text{N} + \text{CsTf}_2\text{N}$ mixtures in the compositions of $x_{\text{LiTf}_2\text{N}} = 1.00, 0.80, 0.50, 0.20,$ and 0 . The XRD patterns of LiTf_2N are not observed for the compositions of $x_{\text{LiTf}_2\text{N}} < 0.50$. The patterns of CsTf_2N are not observed at the compositions of $x_{\text{LiTf}_2\text{N}} > 0.50$. The pattern for the mixed salt of $(x_{\text{LiTf}_2\text{N}}, x_{\text{CsTf}_2\text{N}}) = (0.50, 0.50)$ is different from those for LiTf_2N and CsTf_2N . Thus, it is concluded that an intermediate compound, $\text{LiCs}(\text{Tf}_2\text{N})_2$, is formed at this composition.

In the XRD charts of other binary systems, all the peaks were assigned to those for the constituent single salts. Thus, it is concluded that there is no intermediate compound in other binary

* Corresponding author. E-mail: hagiwara@energy.kyoto-u.ac.jp.

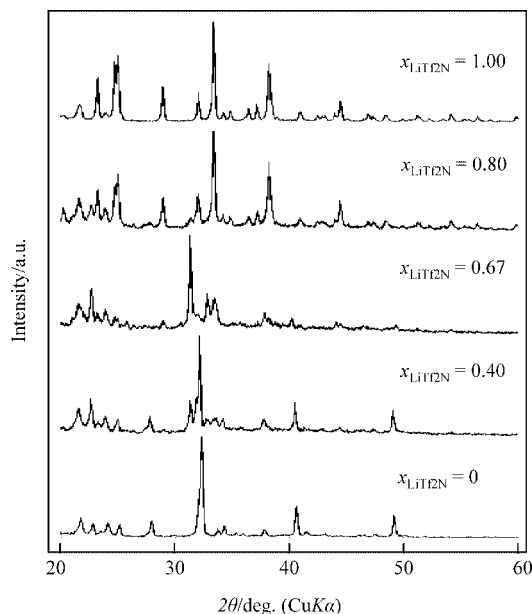
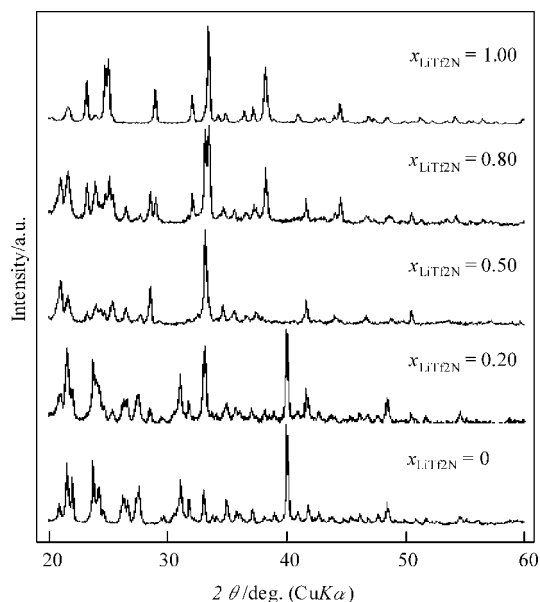
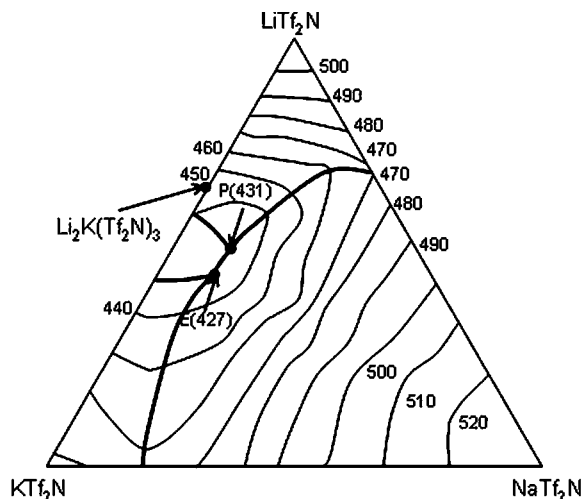
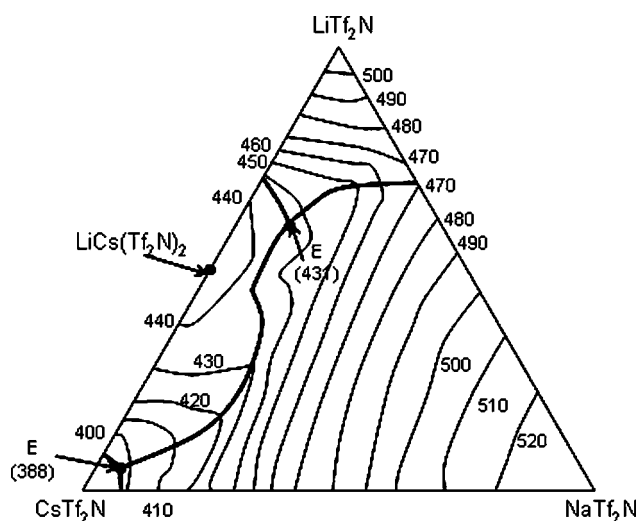
Figure 1. XRD charts of $\text{LiTf}_2\text{N} + \text{KTf}_2\text{N}$ systems.Figure 2. XRD charts of $\text{LiTf}_2\text{N} + \text{CsTf}_2\text{N}$ systems.

Table 1. Reported and Revised Eutectic Compositions x_{eu} , Eutectic Temperatures T_{eu} , and Intermediate Compound for the Binary MTf_2N Salt Mixtures

system	previous study ⁶		present study		compound
	x_{eu}	T_{eu}/K	x_{eu}	T_{eu}/K	
$\text{LiTf}_2\text{N} + \text{NaTf}_2\text{N}$	$x_{\text{LiTf}_2\text{N}} = 0.67$	453	$x_{\text{LiTf}_2\text{N}} = 0.67$	459	-
$\text{LiTf}_2\text{N} + \text{KTf}_2\text{N}$	$x_{\text{LiTf}_2\text{N}} = 0.43$	423	$x_{\text{LiTf}_2\text{N}} = 0.43$	429	$\text{Li}_2\text{K}(\text{Tf}_2\text{N})_3$
$\text{LiTf}_2\text{N} + \text{CsTf}_2\text{N}$	$x_{\text{LiTf}_2\text{N}} = 0.07$	385	$x_{\text{LiTf}_2\text{N}} = 0.07$	391	$\text{LiCs}(\text{Tf}_2\text{N})_2$
	$= 0.6$	432	$= 0.7$	434	-
$\text{NaTf}_2\text{N} + \text{KTf}_2\text{N}$	$x_{\text{NaTf}_2\text{N}} = 0.25$	456	$x_{\text{NaTf}_2\text{N}} = 0.25$	456	-
$\text{NaTf}_2\text{N} + \text{CsTf}_2\text{N}$	$x_{\text{NaTf}_2\text{N}} = 0.07$	383	$x_{\text{NaTf}_2\text{N}} = 0.07$	392	-

and ternary MTf_2N ($M = \text{Li}, \text{Na}, \text{K}, \text{Cs}$) systems. Table 1 summarizes eutectic compositions, eutectic temperatures, and the intermediate compounds for the binary MTf_2N salt mixtures. Eutectic temperatures have been redetermined by the step

Figure 3. Phase diagram of the $\text{LiTf}_2\text{N} + \text{NaTf}_2\text{N} + \text{KTf}_2\text{N}$ system.Figure 4. Phase diagram of the $\text{LiTf}_2\text{N} + \text{NaTf}_2\text{N} + \text{CsTf}_2\text{N}$ system.

heating method in the present study. They are the same as, or slightly higher than, the old values.

Phase Diagrams of Ternary MTf_2N Mixed Salts. The ternary phase diagrams have been constructed for $\text{LiTf}_2\text{N} + \text{NaTf}_2\text{N} + \text{KTf}_2\text{N}$, $\text{LiTf}_2\text{N} + \text{NaTf}_2\text{N} + \text{CsTf}_2\text{N}$, $\text{LiTf}_2\text{N} + \text{KTf}_2\text{N} + \text{CsTf}_2\text{N}$, and $\text{NaTf}_2\text{N} + \text{KTf}_2\text{N} + \text{CsTf}_2\text{N}$ systems. In the diagrams, liquidus curves are shown as a contour map. Temperatures are given in K, and the following abbreviations are used: E, eutectic point; P, peritectic point; M, the lowest melting point in each system.

Figure 3 shows a phase diagram of the $\text{LiTf}_2\text{N} + \text{NaTf}_2\text{N} + \text{KTf}_2\text{N}$ ternary system. The $\text{LiTf}_2\text{N} + \text{KTf}_2\text{N}$ binary subsystem has one peritectic point and one eutectic point. At $(x_{\text{LiTf}_2\text{N}}, x_{\text{NaTf}_2\text{N}}, x_{\text{KTf}_2\text{N}}) = (0.45, 0.10, 0.45)$, the melting temperature, 427 K, is lower than those of the neighboring compositions. Thus, the point is regarded as the ternary eutectic point in the system. This system is a eutectic type, which is reasonably explained from the fact that the binary subsystems are all eutectic type. This ternary system has a composition range that has lower melting points than those of binary subsystems.

Figure 4 shows a phase diagram of the $\text{LiTf}_2\text{N} + \text{NaTf}_2\text{N} + \text{CsTf}_2\text{N}$ ternary system. An intermediate compound, $\text{LiCs}(\text{Tf}_2\text{N})_2$, divides this ternary system into two ternary subsystems, $\text{LiTf}_2\text{N} + \text{NaTf}_2\text{N} + \text{LiCs}(\text{Tf}_2\text{N})_2$ and $\text{LiTf}_2\text{N} + \text{LiCs}(\text{Tf}_2\text{N})_2 + \text{CsTf}_2\text{N}$. In the former subsystem, the point of $(x_{\text{LiTf}_2\text{N}},$

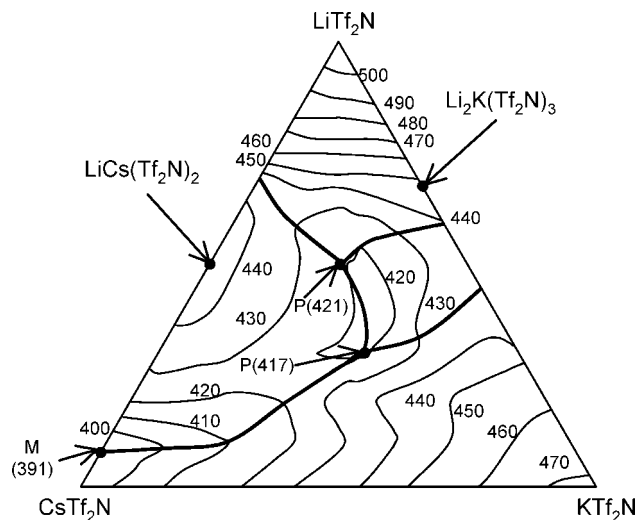


Figure 5. Phase diagram of the $\text{LiTf}_2\text{N} + \text{KTF}_2\text{N} + \text{CsTf}_2\text{N}$ system.

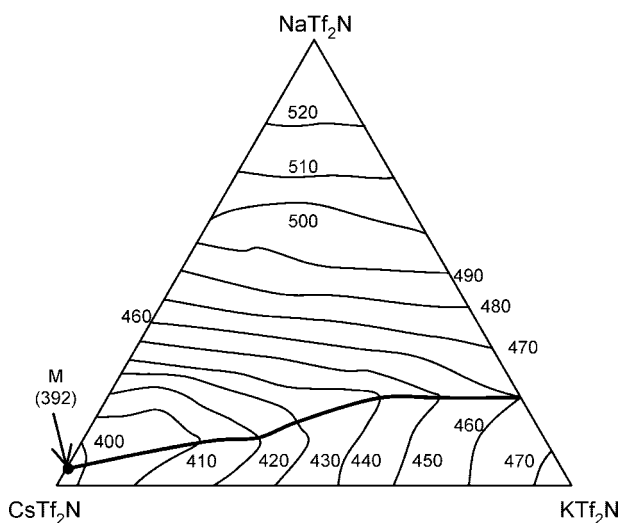


Figure 6. Phase diagram of the $\text{NaTf}_2\text{N} + \text{KTF}_2\text{N} + \text{CsTf}_2\text{N}$ system.

$x_{\text{NaTf}_2\text{N}}, x_{\text{CsTf}_2\text{N}} = (0.60, 0.10, 0.30)$ is considered to be the ternary eutectic point because its melting point, 431 K, is lower than those of the surrounding compositions. In the latter subsystem, the melting temperature, 388 K, at $(x_{\text{LiTf}_2\text{N}}, x_{\text{NaTf}_2\text{N}}, x_{\text{CsTf}_2\text{N}}) = (0.05, 0.05, 0.90)$ is lower than those of the neighboring compositions. Thus, the point is the ternary eutectic point in the subsystem. This ternary system also has the composition ranges that possess lower melting points than those of binary subsystems.

Figure 5 shows a phase diagram of the $\text{LiTf}_2\text{N} + \text{KTF}_2\text{N} + \text{CsTf}_2\text{N}$ ternary system. No ternary eutectic point is found in this system. The lowest melting point is the eutectic point of the binary $\text{LiTf}_2\text{N} + \text{CsTf}_2\text{N}$ system. However, it was found that the ternary mixed salt of $(x_{\text{LiTf}_2\text{N}}, x_{\text{KTF}_2\text{N}}, x_{\text{CsTf}_2\text{N}}) = (0.20, 0.10, 0.70)$ has a lower melting temperature than the binary mixed salt of $(x_{\text{LiTf}_2\text{N}}, x_{\text{CsTf}_2\text{N}}) = (0.20, 0.80)$ containing the same amount of lithium salts. The ternary mixed salt $(x_{\text{LiTf}_2\text{N}}, x_{\text{KTF}_2\text{N}}, x_{\text{CsTf}_2\text{N}}) = (0.20, 0.10, 0.70)$ has been investigated as an electrolyte for lithium secondary batteries operating at intermediate temperature.⁷ In this study, the $\text{Li}/(x_{\text{LiTf}_2\text{N}}, x_{\text{KTF}_2\text{N}}, x_{\text{CsTf}_2\text{N}}) = (0.20, 0.10, 0.70)/\text{LiFePO}_4$ cell showed excellent charge-discharge properties at 423 K.

Figure 6 shows a phase diagram of the $\text{NaTf}_2\text{N} + \text{KTF}_2\text{N} + \text{CsTf}_2\text{N}$ ternary system. Again, no ternary eutectic point is observed in this system, which coincides with the previous report

Table 2. Compositions, x , and Temperatures, T , for Eutectic, Peritectic, and the Lowest Melting Points of the Ternary MTf_2N Salt Mixtures^a

system	$x_{\text{MTf}_2\text{N}}$	T/K
$\text{LiTf}_2\text{N} + \text{NaTf}_2\text{N} + \text{KTF}_2\text{N}$	E: $x_{\text{LiTf}_2\text{N}} = 0.45, x_{\text{NaTf}_2\text{N}} = 0.10, x_{\text{KTF}_2\text{N}} = 0.45$	427
	P: $x_{\text{LiTf}_2\text{N}} = 0.50, x_{\text{NaTf}_2\text{N}} = 0.10, x_{\text{KTF}_2\text{N}} = 0.40$	431
$\text{LiTf}_2\text{N} + \text{NaTf}_2\text{N} + \text{CsTf}_2\text{N}$	E: $x_{\text{LiTf}_2\text{N}} = 0.60, x_{\text{NaTf}_2\text{N}} = 0.10, x_{\text{CsTf}_2\text{N}} = 0.30$	431
	E: $x_{\text{LiTf}_2\text{N}} = 0.05, x_{\text{NaTf}_2\text{N}} = 0.05, x_{\text{CsTf}_2\text{N}} = 0.90$	388
$\text{LiTf}_2\text{N} + \text{KTF}_2\text{N} + \text{CsTf}_2\text{N}$	P: $x_{\text{LiTf}_2\text{N}} = 0.50, x_{\text{KTF}_2\text{N}} = 0.25, x_{\text{CsTf}_2\text{N}} = 0.25$	421
	P: $x_{\text{LiTf}_2\text{N}} = 0.30, x_{\text{KTF}_2\text{N}} = 0.40, x_{\text{CsTf}_2\text{N}} = 0.30$	417
	M: $x_{\text{LiTf}_2\text{N}} = 0.07, x_{\text{KTF}_2\text{N}} = 0, x_{\text{CsTf}_2\text{N}} = 0.93$	391
$\text{NaTf}_2\text{N} + \text{KTF}_2\text{N} + \text{CsTf}_2\text{N}$	M: $x_{\text{NaTf}_2\text{N}} = 0.07, x_{\text{KTF}_2\text{N}} = 0, x_{\text{CsTf}_2\text{N}} = 0.93$	392

^a E, eutectic; P, peritectic; M, the lowest melting.

Table 3. Thermal Decomposition Temperatures, T_d , of MTf_2N Ternary Mixtures

system	$x_{\text{MTf}_2\text{N}}$	T_d/K
$\text{LiTf}_2\text{N} + \text{NaTf}_2\text{N} + \text{KTF}_2\text{N}$	$x_{\text{LiTf}_2\text{N}} = 0.45, x_{\text{NaTf}_2\text{N}} = 0.10, x_{\text{KTF}_2\text{N}} = 0.45$	660
$\text{LiTf}_2\text{N} + \text{NaTf}_2\text{N} + \text{CsTf}_2\text{N}$	$x_{\text{LiTf}_2\text{N}} = 0.30, x_{\text{NaTf}_2\text{N}} = 0.30, x_{\text{CsTf}_2\text{N}} = 0.40$	661
$\text{LiTf}_2\text{N} + \text{KTF}_2\text{N} + \text{CsTf}_2\text{N}$	$x_{\text{LiTf}_2\text{N}} = 0.30, x_{\text{KTF}_2\text{N}} = 0.30, x_{\text{CsTf}_2\text{N}} = 0.40$	661
$\text{NaTf}_2\text{N} + \text{KTF}_2\text{N} + \text{CsTf}_2\text{N}$	$x_{\text{NaTf}_2\text{N}} = 0.30, x_{\text{KTF}_2\text{N}} = 0.30, x_{\text{CsTf}_2\text{N}} = 0.40$	710

that no eutectic point was found in the binary $\text{KTF}_2\text{N} + \text{CsTf}_2\text{N}$ system.⁶ The lowest melting point is the binary $\text{NaTf}_2\text{N} + \text{CsTf}_2\text{N}$ eutectic point. No intermediate compound was found in this system. Thus, this diagram has a simple feature: a canyon of low liquidus temperatures runs from the binary eutectic point of $\text{NaTf}_2\text{N} + \text{KTF}_2\text{N}$ to that of $\text{NaTf}_2\text{N} + \text{CsTf}_2\text{N}$.

Table 2 summarizes the compositions and temperatures for eutectic, peritectic, and the lowest melting points of these systems.

Finally, the thermal decomposition temperatures of four selected ternary mixtures were summarized in Table 3. It was confirmed by TG measurements that the lowest decomposition temperature of one of the constituent single salts determines the thermal decomposition temperature of each binary and ternary system. Thus, there is no effect of the mixing of MTf_2N salts on the decomposition temperatures except for incongruent melting of the intermediate compound.

Conclusions

For binary MTf_2N ($M = \text{Li}, \text{Na}, \text{K}, \text{Cs}$) systems, eutectic temperatures have been revised, and existences of intermediate compounds, $\text{Li}_2\text{K}(\text{Tf}_2\text{N})_3$ and $\text{LiCs}(\text{Tf}_2\text{N})_2$, have been confirmed. Four ternary phase diagrams have been constructed for ternary MTf_2N ($M = \text{Li}, \text{Na}, \text{K}, \text{Cs}$) salt mixtures. Some ternary mixed MTf_2N melts are expected to be more useful than the single and binary MTf_2N melts for practical applications as electrolytes in the electrochemical devices owing to their low melting temperatures with higher lithium or sodium content.

Supporting Information Available:

The tables of data for Figures 3 to 6. This material is available free of charge via the Internet at <http://pubs.acs.org>.

Literature Cited

- Lascaud, S.; Perrier, M.; Vallée, A.; Besner, S.; Prud'homme, J.; Armand, J. Phase Diagrams and Conductivity Behavior of Poly(Ethylene

- Oxide)-Molten Salt Rubbery Electrolytes. *Macromolecules* **1994**, *27*, 7469–7477.
- (2) Foropoulos, J.; DesMarteau, D. D. Synthesis, Properties, and Reactions Bis(trifluoromethylsulfonyl)Imide, $(\text{CF}_3\text{SO}_2)_2\text{NH}$. *Inorg. Chem.* **1984**, *23*, 3720–3723.
- (3) Matsumoto, H.; Yanagida, M.; Tanimoto, K.; Kojima, T.; Tamiya, Y.; Miyazaki, Y. Improvement of Ionic Conductivity of Room Temperature Molten Salt Based on Quaternary Ammonium Cation and Imide Anion. *Proc. Electrochem. Soc.* **2000**, *99-41*, 186–192.
- (4) Koura, N.; Etoh, K.; Idemoto, Y.; Matsumoto, F. Electrochemical Behavior of Graphite-Lithium Intercalation Electrode in AlCl_3 -EMIC-LiCl-SOCl₂ Room-Temperature Molten Salt. *Chem. Lett.* **2001**, 1320–1321.
- (5) Sakaebe, H.; Matsumoto, H. N-Methyl-N-Propylpiperidinium Bis(Tri-fluoromethanesulfonyl)Imide (PP13-TFSI) - Novel Electrolyte Base for Li Battery. *Electrochem. Commun.* **2003**, *5*, 594–598.
- (6) Hagiwara, R.; Tamaki, K.; Kubota, K.; Goto, T.; Nohira, T. Thermal properties of mixed alkali bis(trifluoromethylsulfonyl)amides. *J. Chem. Eng. Data* **2008**, *53* (2), 355–358.
- (7) Watarai, A.; Kubota, K.; Yamagata, M.; Goto, T.; Nohira, T.; Hagiwara, R.; Ui, K.; Kumagai, N. A rechargeable lithium metal battery operating at intermediate temperatures using molten alkali bis(trifluoromethylsulfonyl)amide mixture as an electrolyte. *J. Power Sources*, **2008**, *183*, 724–729.

Received for review April 26, 2008. Accepted July 14, 2008. This work was financially supported by a Grant in Aid for Scientific Research for Priority Area “Science of Ionic Liquids” from Japanese Ministry of Education, Culture, Sports, Science and Technology.

JE800292F